

Bulk and Surface Structures of V₂O₅/ZrO₂ Systems and Their Relevance for *o*-Xylene Oxidation

C. L. Pieck,^{*,†} S. del Val, M. López Granados, M. A. Bañares, and J. L. G. Fierro

Instituto de Catálisis y Petroleoquímica, CSIC, Cantoblanco, E-28049 Madrid, Spain

Received September 21, 2001. In Final Form: January 10, 2002

Zirconia-supported vanadium oxide systems, with V₂O₅ loadings ranging from V/Zr = 0.033–0.270 atom ratios (0.2–2 monolayers), were prepared by impregnation of a porous ZrO₂ substrate with ammonium metavanadate solutions. The surface structures of air-calcined samples were elucidated by Raman and X-ray photoelectron spectroscopic techniques and thermal desorption methods. Some insight into how the bulk structures of these materials developed upon thermal treatment was derived from the X-ray diffraction patterns and temperature-programmed reduction. At low V content, surface-dispersed vanadium oxide species were formed, which produced the transformation of the ZrO₂ support from the tetragonal phase into the monoclinic one. At higher vanadium oxide contents, a solid-state reaction between V₂O₅ and ZrO₂ occurred, with subsequent formation of the ZrV₂O₇ phase, this being the major V-containing phase. The reactivity of these surface structures was examined by looking at their performance for the oxidation of *o*-xylene to phthalic anhydride. Activity tests indicated that surface vanadium oxide species were more active for the oxidation of *o*-xylene but had a lower selectivity to phthalic anhydride.

Introduction

Phthalic anhydride is currently obtained industrially via the selective oxidation of *o*-xylene. This is a complex reaction that involves the participation of 12 electrons, the abstraction of 6 hydrogen atoms, and the incorporation of 3 oxygen atoms in the *o*-xylene molecule. Curiously, however, it is achieved in a single reaction process with high selectivity to the desired product at total conversion.^{1,2} The key to this achievement is the use of a V₂O₅/TiO₂ catalyst. In any case, some intermediate products—such as *o*-tolualdehyde, phthalide, and maleic anhydride—and deep oxidation products (CO and CO₂) are also found among the reaction products.^{1–5} Some authors have also reported the formation of polymerization products, which are a consequence of the strong adsorption of *o*-xylene molecules and intermediate products on the catalyst surface. These deposits have been reported to decrease the selectivity to phthalic anhydride and would be an additional source of CO_x.^{2,6,7} The oxidation of *o*-xylene has been the subject of several kinetic studies and many reaction mechanisms have been proposed.^{3,8–10} It is assumed that the reaction takes place through a Mars–van Krevelen mechanism, involving a reduction–oxidation

cycle of the active species. There is currently broad consensus that the formation of phthalic anhydride occurs in consecutive steps, starting with the adsorption of the reactant molecules, followed by the formation of intermediate products, which can also be detected in the gas phase. The formation of CO_x can take place at any stage of the reaction. CO and CO₂ are formed from the deep oxidation of *o*-xylene, the intermediate products, or directly from phthalic anhydride.

The first catalyst used at commercial scale for the oxidation of *o*-xylene to phthalic anhydride was V₂O₅,^{11,12} which was replaced by V₂O₅/TiO₂ (anatase) at the end of the 1960s.¹ The vanadium content was 2–15%, and it has been demonstrated that selectivity is higher when the V is highly dispersed and does not form V₂O₅ crystals.¹ The promoting effect of titania in the oxidation of *o*-xylene has been attributed to an increase in the number of V=O bonds and to their weakening.⁹ The best performance is obtained when a bidimensional monolayer of V-supported species on the oxide is attained.^{13,14}

Ti shares its place in the IVb group of the periodic table with Zr and Hf, elements that have similar electronic properties. In the past few years, and especially in the case of Zr, zirconia-based materials have attracted the interest of the scientific community for different catalytic uses such as isomerization of light hydrocarbons,¹⁵ toluene oxidation,¹⁶ oxidative dehydrogenation,¹⁷ three-way catalysts,¹⁸ fuel cells and electrocatalysis,¹⁹ etc. The successful oxidation of *o*-xylene to phthalic anhydride has been

* To whom correspondence should be addressed at Instituto de Investigaciones en Catálisis y Petroquímica (INCAPE), Santiago del Estero 2654, 3000 Santa Fe, Argentina. Tel: +54-342-4555279. Fax: +54-342-4531068. E-mail: pieck@fiqus.unl.edu.ar.

† On leave from INCAPE (FIQ-UNL, CONICET), Santiago del Estero 2654, 3000 Santa Fe, Argentina.

(1) Nikolov, V.; Klissurski D.; Anastasov, A. *Catal. Rev. Sci. Eng.* **1991**, *33*, 319–374.

(2) Dias, C. R.; Portela, M. F.; Bond, G. C. *Catal. Rev. Sci. Eng.* **1997**, *39*, 169–207.

(3) Saleh, R. Y.; Wachs, I. E. *Appl. Catal.* **1987**, *31*, 87–98.

(4) Centi, G.; Pinelli, D.; Trifirò, F. *J. Mol. Catal.* **1990**, *59*, 221–232.

(5) Ivanoskaya, F. A.; Sembayev, D. K. *React. Kinet. Catal. Lett.* **1991**, *45*, 107–110.

(6) Dias, C. R.; Portela, M. F.; Bond, G. C. *J. Catal.* **1995**, *157*, 353–358.

(7) Dias, C. R.; Portela, M. F.; Bond, G. C. *J. Catal.* **1996**, *162*, 284–294.

(8) Bond, G. C. *J. Chem. Technol. Biotechnol.* **1997**, *68*, 6–13.

(9) Dias, C. R.; Portela, M. F.; Bond, G. C. *J. Catal.* **1995**, *157*, 344–352.

(10) Bond, G. C. *J. Catal.* **1989**, *116*, 531–539.

(11) Nikolov, V.; Radkov, R.; Jurov, B.; Georgiev, S.; Gerogiev, L. *Khim. Ind.* **1983**, *2*, 74–78.

(12) Sutter, H. *Phthalsäureanhydride*; Verlag: München, 1973.

(13) Wachs, I. E.; Saleh, R. Y.; Chan, S. S.; Chersich, C. C. *Appl. Catal.* **1985**, *15*, 339–352.

(14) Gasior, M.; Gasior, I.; Grzybowska, B. *Appl. Catal.* **1984**, *10*, 87–100.

(15) Parera, J. M. *Catal. Today* **1992**, *15*, 481–490.

(16) Sanati, M.; Andersson, A.; Wallenberg, L. R.; Rebenstorf, B. *Appl. Catal., A* **1993**, *106*, 51–72.

(17) Khodakov, A.; Yang, J.; Su, S.; Iglesia, E.; Bell, A. T. *J. Catal.* **1998**, *177*, 343–351.

(18) Balducci, G.; Fornasiero, P.; Graziani, G. *Catal. Lett.* **1995**, *33*, no 1/2, 193–200.

(19) Vayenas, C. G.; Bebelis, S. *Catal. Today* **1999**, *51*, 581–594.

reported for V_2O_5/ZrO_2-TiO_2 catalysts.²⁰ Titania and zirconia are also the supports required for the preparation of solid superacids, e.g., $SO_4^{2-}-ZrO_2$ and $SO_4^{2-}-TiO_2$: materials with an acidity far in excess of 100% H_2SO_4 .²¹

In this work we attempted to assess the potential of V_2O_5/ZrO_2 materials as alternative catalysts for the oxidation of *o*-xylene to phthalic anhydride. Zirconia was chosen for the study mainly because of its similarity with titania but also because it is stable in both reducing and oxidizing atmospheres and has four different kinds of sites: oxidizing, reducing, acid, and basic.²² Apart from serving as a support for the active V species, the oxidizing and reducing sites in zirconia could be useful for the target reaction and noticeable effects on the activity and selectivity were found.

Experimental Section

Sample Preparation. *Support.* $Zr(OH)_4$ stabilized with 3.5% SiO_2 was supplied by MEL Chemicals. The material was calcined in air at 650 °C for 4 h in order to obtain crystalline ZrO_2 .

V_2O_5/ZrO_2 Catalysts. The catalysts were prepared in a Büchi 461 rotary evaporator. Four grams of ZrO_2 was first immersed in a distilled water- HNO_3 solution (pH = 2). Then, the desired amount of NH_4VO_3 was dissolved and the solution was heated to 80 °C at a reduced pressure of 0.7 bar until dryness. A dry powder was obtained at the end. The samples were then dried in an oven at 120 °C overnight and finally calcined in air at 650 °C for 4 h. Samples with different V/Zr atomic ratios (0.033, 0.082, 0.135, and 0.270) were prepared in this way. The ratios correspond to 0.2-, 0.5-, 1.0-, and 2.0-fold the dispersion limit of vanadium oxide on zirconia.

Zirconium Vanadate. ZrV_2O_7 was prepared to serve as a reference. It was prepared by mixing an aqueous solution of NH_4VO_3 with a stoichiometric amount of ZrO_2 in order to obtain a V/Zr atomic ratio of 2. The excess water was eliminated in a rotary evaporator by heating at 80 °C under reduced pressure (0.7 bar). The sample was then dried in an oven at 120 °C overnight and finally calcined at 700 °C for 24 h.

Characterization. *Specific Surface.* Nitrogen adsorption isotherms (-196 °C) were recorded on an automatic Micromeritics ASAP-2000 apparatus. Prior to the adsorption experiments, the samples were outgassed at 140 °C for 2 h. BET areas were computed from the adsorption isotherms ($0.05 < P/P_0 < 0.27$). A value of 0.164 nm² for the cross section of the adsorbed N_2 molecule at -196 °C was adopted.

Raman Spectroscopy. Raman spectra were obtained on a Renishaw system 1000 apparatus equipped with a single monochromator, a CCD detector cooled at -73 °C, and a holographic super-Notch filter. The latter filters the elastic scattering so that the Raman signal remains higher than when triple monochromator spectrometers are used. The samples were excited with a 514 nm Ar laser. Spectral resolution was ca. 4 cm⁻¹, and spectrum acquisition consisted of 10 30-s accumulations. The spectra were obtained under dehydrated conditions (ca. 120 °C) in a hot stage plate (Linkam TS-1500) in a flow of dry air. Hydrated samples were obtained at room temperature after and during exposure to a stream of humid synthetic air.

X-ray Diffraction (XRD). XRD spectra were recorded on a Siemens Krystalloflex D-500 diffractometer, using $Cu K\alpha$ radiation ($\lambda = 0.15418$ nm) and a graphite monochromator. Working conditions were 40 kV, 30 mA (1200 W), and a scan rate of 2°/min for Bragg angles (2θ) from 5 to 70°.

Temperature-Programmed Reduction. A Micromeritics TPR/TPD 2900 apparatus equipped with a thermal conductivity detector was used. The reducing mixture was 5% H_2 in argon. The flow rate was 50 cm³/min, and the heating rate was 10 °C/min. The samples were previously treated in He at 150 °C for 1 h in order to eliminate the humidity present.

Table 1. BET Specific Area and Total Acidity As Measured by NH_3 Adsorption

V/Zr atomic ratio	monolayers	BET area (m ² /g)	NH_3 (au)/m ²	NH_3/V (au)
0		86	0.81	
0.033	0.2	62	1.31	24.6
0.082	0.5	19	2.18	5.05
0.135	1	10	2.70	2.00
0.270	2	7	0.49	0.13
ZrV_2O_7		<1	0.00	

X-ray Photoelectron Spectroscopy. Photoelectron spectra were recorded with a VG Escalab 200R electron spectrometer equipped with a hemispherical electron analyzer, using an Mg $K\alpha$ ($h\nu = 1253.6$ eV) X-ray source. The energy regions of V2p-O1s, Zr3d, and C1s levels were scanned at a pass energy of 20 eV and signal-averaged for 90 scans. These conditions are appropriate for obtaining good signal-to-noise ratios. A PDP 11/04 computer (Digital) was used to record and analyze the spectra. Peak intensities were estimated by calculating the integral of each peak after subtraction of an S-shaped background and fitting the experimental curve to a combination of Gaussian and Lorentzian lines. The C1s peak (contamination) at a binding energy (BE) of 284.9 eV was taken as an internal standard for BE measurements. Surface atomic ratios were determined from the intensity ratios normalized by atomic sensitivity factors.²³

Ammonia Temperature-Programmed Desorption (TPD- NH_3). The gases evolved during the TPD test were analyzed using a mass spectrometer connected in series (Balzers QMG 421C quadrupole). The samples were first treated at 500 °C with a mixture of 8% oxygen in He for 2 h. Then, NH_3 was adsorbed at 120 °C for 150 min from a flowing mixture of 5% NH_3 in He. Finally, the temperature was raised at a rate of 10 °C/min and a stream of pure He was injected into the reactor. The desorbed species were analyzed on-line.

*Reaction of *o*-Xylene Oxidation.* Catalytic activity measurements were carried out in a plug-flow glass fixed-bed reactor heated by means of a cylindrical oven in a previously described apparatus.²⁴ The reactor catalyst load consisted of 0.25 g of catalyst diluted seven times in silicon carbide (0.42–0.50 mm). W/F was 179 g·s/L. The molar concentrations of *o*-xylene and oxygen in the feed were 0.8 and 20.8%, respectively (78.4% nitrogen). The inlet lines were heated to 180 °C in order to ensure the evaporation of *o*-xylene. An ice-bath trap was placed between the GC and the reactor outlet to condense part of the products. The lines connecting the reactor and the trap were heated to 250 °C. The temperature of the bottom part of the reactor, downstream from the catalyst bed, was higher than 350 °C.

Results and Discussion

Table 1 shows the variation in specific area as a function of the V/Zr atomic ratio of the catalysts. The V-free support has a specific surface area of 86 m²/g. The area decreases after loading small amounts of V, but at higher V contents it drops markedly. According to Su and Bell²⁵ and Sohn et al.,²⁶ after calcination at 500 and 400 °C, respectively, and at low vanadia coverages, the BET area of vanadia/zirconia systems prepared on $Zr(OH)_4$ increases. Our catalysts, calcined at 650 °C, show a moderate value of the BET area. The area decreases at low vanadia coverage and is subject to a strong decrease as the V/Zr ratio approaches 0.082. Su and Bell reported a decrease in the BET area as the V coverage approaches the monolayer state.²⁵ However, Sohn et al. failed to detect any decrease in the BET values beyond the V monolayer coverage.²⁶ This may be due to the lower calcination temperature

(23) Wagner, C. D.; Davis, L. E.; Zeller, M. V.; Taylor, J. A.; Raymond, R. H.; Gale, L. H. *Surf. Interface Anal.* **1981**, *3*, 211–225.

(24) del Val, S.; López Granados, M.; Fierro, J. L. G.; Santamaría-González, J.; Jiménez-López, A. *J. Catal.* **1999**, *188*, 203–214.

(25) Su, S. C.; Bell, A. T. *J. Phys. Chem. B* **1998**, *102*, 7000–7007.

(26) Sohn, J. R.; Cho, S. G.; Pae, Y. I.; Hayashi, S. *J. Catal.* **1996**, *159*, 170–177.

(20) Saleh, R. Y.; Wachs, I. E. US Patent 4,728,744, 1988.

(21) Yadav, G. D.; Nair, J. J. *Microporous Mesoporous Mater.* **1991**, *33*, 1–48.

(22) Nakano, Y.; Iizuka, T.; Hattori, H.; Tanabe, K. *J. Catal.* **1979**, *57*, 1–10.

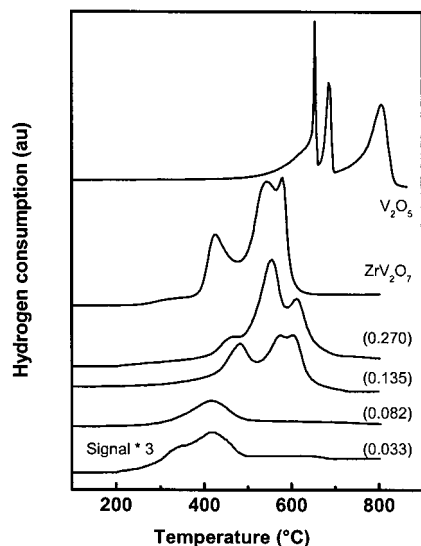
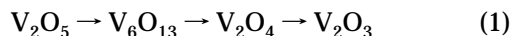


Figure 1. Temperature-programmed reduction plots of V_2O_5/ZrO_2 catalysts, ZrV_2O_7 , and V_2O_5 .

used in that case (400 °C), which precludes many transformations from taking place at higher temperatures.²⁵ Therefore the differences must be due to the different calcination temperatures used.

Figure 1 shows the TPR plots for the pure oxide (V_2O_5), the reference ZrV_2O_7 , and the prepared V_2O_5/ZrO_2 catalysts. The TPR plot of the V_2O_5 sample has three reduction peaks. Similar results have been reported by Bond et al.,²⁷ Bosch et al.²⁸ and Koranne et al.²⁹ The three peaks have been attributed to the following reduction steps:^{28,29}



The pattern of hydrogen consumption is consistent with the reported mechanism (the sum of the area of the first and the second peaks is equal to that of the third). ZrV_2O_7 displays three reduction peaks at lower temperatures than those of V_2O_5 . It should be noted that for the V_2O_5/ZrO_2 catalysts V is reduced at a lower temperature than in pure bulk V_2O_5 . It can also be seen that at low V contents only one peak near 400 °C is detected. This must be related to the reduction of surface-dispersed vanadium oxide species. Peaks at higher temperatures are due to bulk crystalline V species.²⁹ At higher V contents, there is a shift of the reduction peaks to higher temperatures. For V/Al_2O_3 catalysts, it has been reported that at increasing coverage the peak due to crystalline V_2O_5 shifts to higher temperatures, approaching the reduction temperature of pure V_2O_5 .³⁰ The large difference in the reduction temperatures of V/ZrO_2 catalysts and V_2O_5 found in the TPR profiles of VO_x/ZrO_2 samples indicates that no, or at least very little, V_2O_5 is present.

Figure 2 shows the TPD profiles of NH_3 from the support and from the V_2O_5/ZrO_2 catalysts. A blank experiment using ZrV_2O_7 shows no adsorption of ammonia. V-free ZrO_2 has a broad peak of desorption of NH_3 that can be attributed to a distribution of sites of different acid

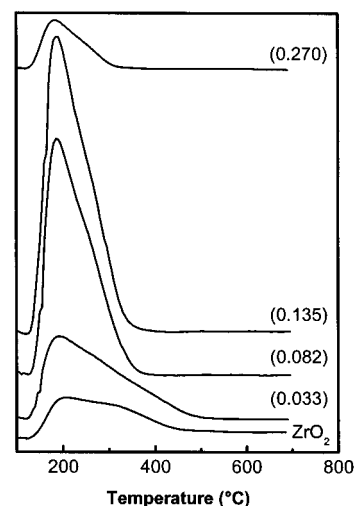


Figure 2. Temperature-programmed desorption of NH_3 on V_2O_5/ZrO_2 catalysts and V-free ZrO_2 .

strengths of both the Lewis and Brønsted type.³¹ For the supported VO_x/ZrO_2 samples, it can be seen that the amount of desorbed NH_3 increases with increasing V/Zr surface ratios up to V/Zr = 0.135, thereafter decreasing. The data reported in Table 1 indicate the presence of such a maximum per square meter at V/Zr = 0.135. This maximum can be explained tentatively by assuming the progressive formation of the ZrV_2O_7 phase, which has practically no adsorption affinity for NH_3 . The acid sites are assumed to be located at the V–O–support and V–OH–support groups, although in the latter case no spectroscopic evidence of their existence has been found.³² However, the amount of ammonia per vanadium site is maximum for V/Zr = 0.033, where only surface vanadium oxide species are present. When the V/Zr ratio is 0.082, NH_3 adsorption per vanadium site decreases by a factor of 5. In this catalyst, trace amounts of V_2O_5 microcrystallites suggest that no more surface vanadium oxide can be stabilized on zirconia. Thus, the zirconia support must be highly covered. At higher V/Zr ratios, vanadium oxide species are no longer dispersed since the ZrV_2O_7 phase dominates (Raman and XRD data). The surface atomic V/Zr ratio measured by X-ray photoelectron spectroscopy (XPS) reveals a loss of vanadium dispersion on the V/Zr = 0.135 sample. The loss of dispersion of vanadium and the formation of the ZrV_2O_7 phase must account for the decrease in the number of acid sites in the VO_x/ZrO_2 system. The maximum in ammonia adsorption has also been reported by Sohn et al.²⁶ for the V_2O_5/ZrO_2 system. These authors found that the incorporation of V_2O_5 on the ZrO_2 surface generated more acid sites and of greater acid strength than the single components. Thus, the VO_x/ZrO_2 interface must be associated with the generation of new acid sites. The formation of vanadia species on the surface of oxide supports has been shown to be accompanied by a decrease in the number of surface Lewis acid sites and an increase in the number of surface Brønsted acid sites (ref 32 and references therein).

Figure 3 shows the XRD patterns of the V_2O_5/ZrO_2 catalysts, together with that of the V-free support and that of the reference ZrV_2O_7 compound. The V-free support displays a diffraction peak at 30.5°, presumably due to

(27) Bond, G. C.; Perez Zurita, J.; Flamerz, S.; Gellings, P. J.; Bosh, H.; Van Ommen, J. G.; Kip, B. J. *J. Appl. Catal.* **1986**, *22*, 361–378.

(28) Bosch, H.; Kip, B. J.; van Ommen, J. G.; Gellings, P. J. *J. Chem. Soc., Faraday Trans. 1* **1984**, *80*, 2479–2488.

(29) Koranne, M. M.; Goodwin, J. G., Jr.; Marcelin, G. *J. Catal.* **1994**, *148*, 369–377.

(30) Roozeboom, F.; Mittelmeijer-Hazeleger, M. C.; Moulin, J. A.; Medema, J.; de Beer, V. H. J.; Gelling, P. J. *J. Phys. Chem.* **1980**, *84*, 2783–2791.

(31) Tanabe, K.; Misono, M.; Ono, Y.; Hattori, H. In *New Solid Acids and Bases—Their Catalytic Properties*; Kodansha-Elsevier: Tokyo, 1989; Chapter 2.

(32) Wachs, I. E.; Weckhuysen, B. M. *J. Appl. Catal.*, **A** **1997**, *157*, 67–90.

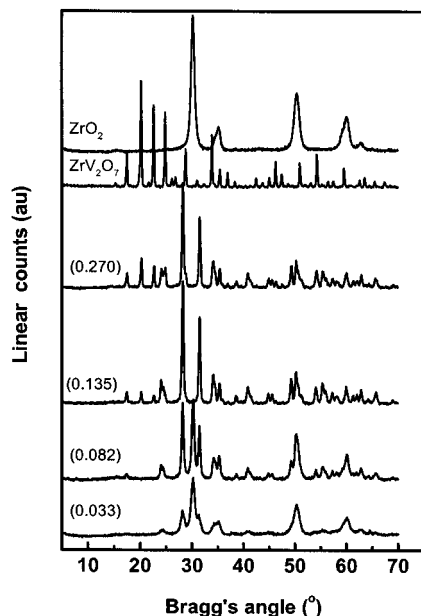


Figure 3. X-ray diffraction spectra of V_2O_5/ZrO_2 catalysts, ZrV_2O_7 and ZrO_2 .

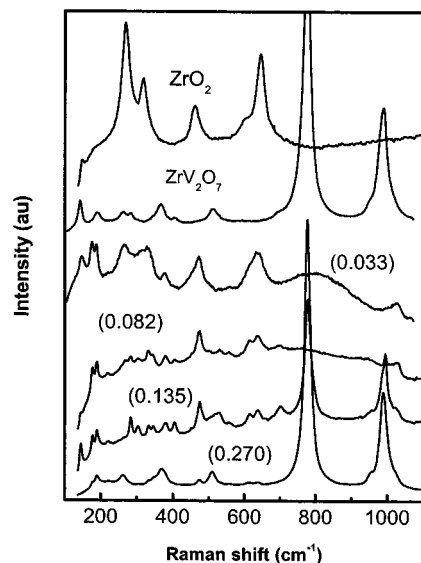


Figure 4. Raman spectra of dehydrated V_2O_5/ZrO_2 catalysts and ZrV_2O_7 and ZrO_2 references.

the presence of the tetragonal (or cubic) phase. However, the absence of diffraction peaks at 28.2 and 31.5° precludes the presence of the monoclinic phase.³³ Incorporation of a small amount of V ($V/Zr = 0.033$) induces a phase transformation in zirconia. At $V/Zr = 0.135$ and at higher V loads, 100% of the monoclinic phase is formed and, simultaneously, diffraction peaks at 16 , 20 , 22.5 , and 24.8° —characteristic of the ZrV_2O_7 phase—are also present.³⁴

Figure 4 shows the Raman spectra of the calcined V_2O_5/ZrO_2 catalysts, ZrO_2 support, and ZrV_2O_7 reference compounds under dehydrated conditions. The V-free support is 100% tetragonal, as indicated by the Raman bands at 263 , 325 , 472 , 608 , and 640 cm^{-1} , in agreement

(33) Selected Power Diffraction Data For Metals and Alloys. *Data Book*, 1st ed.; International Center For Diffraction Data (JCPDS): Swarthmore, PA., Vol. II, cards No. 13-307 and No 24-1164.

(34) Selected Power Diffraction Data For Metals and Alloys. *Data Book*, 1st ed.; International Center For Diffraction Data (JCPDS): Swarthmore, PA., Vol. II, cards No 16-0422.

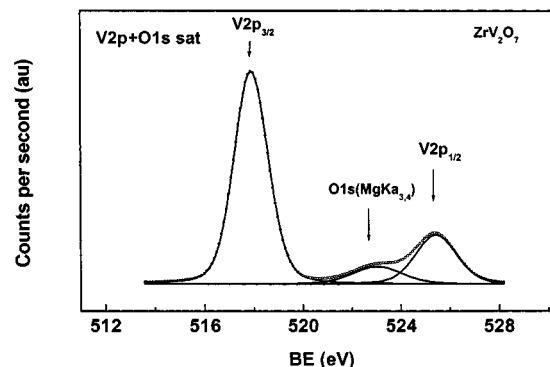


Figure 5. $V2p$ core-level spectrum after background subtraction of bulk ZrV_2O_7 : (○) experimental data points; continuous lines correspond to the fit.

with the XRD patterns. At low vanadia coverage, a transition to the monoclinic phase is evident (new modes near 175 , 190 , and 477 cm^{-1}).³⁵ The Raman band close to 143 cm^{-1} at $V/Zr = 0.033$ does not correspond to crystalline V_2O_5 but rather to the tetragonal ZrO_2 phase, since no other bands of crystalline V_2O_5 are present. The band at 1030 cm^{-1} is sensitive to hydration, confirming that it belongs to dispersed vanadium oxide species since crystals are not sensitive to hydration treatments.³⁶ However, the $V/Zr = 0.082$ sample shows trace amounts of crystalline V_2O_5 (990 cm^{-1}), although the predominant vanadium phase is ZrV_2O_7 . The Raman measurements reveal that vanadia disperses on zirconia support at low VO_x loading (1030 cm^{-1}) and that ZrV_2O_7 is formed as the vanadia loading increases (990 , 780 cm^{-1}). It has been demonstrated that ZrV_2O_7 develops via interaction of dispersed surface vanadia with Zr sites.³⁷

Further insight into the chemical state and dispersion of V oxide on the ZrO_2 substrate was gained using XPS. Since the binding energies (BE) of $V2p$ and $O1s$ core levels are close, a careful analysis of the profile of $V2p$ peaks is required. Figure 5 displays the $V2p$ doublet of the unsupported ZrV_2O_7 compound. The splitting of the two $V2p_{3/2}$ and $V2p_{1/2}$ peaks is approximately 7.3 eV , in agreement with other reports in the literature for V compounds.^{38,39} Exact determination of the BE, specifically that of $V2p_{1/2}$ peak, is difficult due to the interfering $O1s$ satellite component, whose origin lies in the $MgK\alpha_{3,4}$ line. This interfering peak is present in all the spectra since no monochromator was used to filter the X-ray exciting source. Additionally, the resolution of the $V2p_{1/2}$ is much poorer than that of the $V2p_{3/2}$ peak. This can be very complex for $V/Zr = 0.033$ and $V/Zr = 0.082$ samples. Consequently, only the $V2p_{3/2}$ was considered in our calculations, even after background subtraction and peak decomposition procedures.

The BE values of the $V2p_{3/2}$ peak and the relative XPS V/Zr atomic ratios are summarized in Table 2. For the sake of clarity, the $V2p_{3/2}$ core-level spectra for supported $V/Zr = 0.033$, 0.082 , 0.135 , and 0.270 catalysts are displayed in Figure 6. These spectra were satisfactorily fitted to two components: the high BE peak at a BE of $517.6\text{--}517.7\text{ eV}$, and the low BE peak at $516.6\text{--}516.8\text{ eV}$,

(35) Miciukiewicz, J.; Mang, T.; Knözinger, H. *Appl. Catal. A* **1995**, *122*, 151–159.

(36) Wachs, I. E. *Catal. Today* **1996**, *27*, 437–455.

(37) Pieck, C. L.; Bañares, M. A.; Vicente, M. A.; Fierro, J. L. G. *Chem. Mater.* **2001**, *13*, 1174–1180.

(38) Gil Lambias, F. J.; Escudéy, A. M.; Fierro, J. L. G.; Lopez Agudo, A. *J. Catal.* **1986**, *95*, 520–526.

(39) Bond, G. C.; Perez Zurita, J.; Flamerz, S. *Appl. Catal.* **1986**, *27*, 353–362.

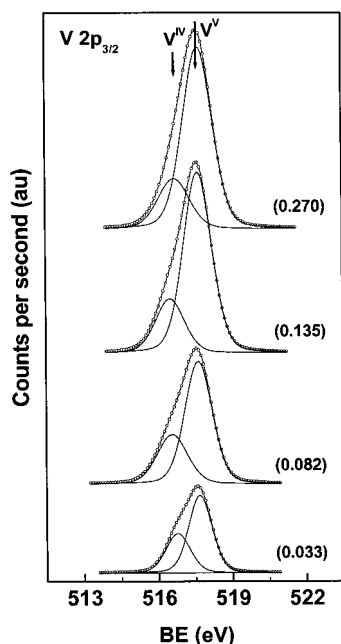


Figure 6. $V2p_{3/2}$ core-level spectra after background subtraction of ZrO_2 -supported vanadia samples: (○) experimental data points; continuous lines correspond to the fit.

Table 2. Binding Energies (eV) of Core Electrons and Surface Atomic Ratios of V_2O_5/ZrO_2 Samples

V/Zr atomic ratio	Zr3d _{5/2}	V2p _{3/2}	V/Zr atom	V ^{IV} /V _{total}
0.033	182.2	517.7	0.129	0.36
		516.8		
0.082	182.2	517.6	0.252	0.32
		516.5		
0.135	182.2	517.6	0.253	0.23
		516.5		
0.270	182.2	517.7	0.354	0.22
		516.7		
ZrV ₂ O ₇	182.4	517.5	3.120	0.00

assigned to V^V and V^{IV} species, respectively.⁴⁰ From the fitting of the experimental peaks, the relative abundance of V^{IV}/V_{total} was also calculated. These values are also summarized in Table 2. According to Figure 6 and the data in Table 2, the proportion of V^{IV} ions decreases upon increasing the V content in the catalysts (from 0.36 in V/Zr = 0.033 to 0.22 in V/Zr = 0.270). This points to the stabilization of a relatively higher proportion of V^{IV} in samples with lower V contents with respect to that containing a higher proportion of V; this is consistent with the greater reducibility of dispersed V oxide species than in multilayered V oxides.^{41,42} By contrast, the V2p_{3/2} peak in the reference ZrV₂O₇ exhibited a single component at 517.5 eV, characteristic of V^V species, as confirmed by Raman spectroscopy.

Surface atomic ratios were also calculated from the XPS peak intensity ratios, normalized by atomic sensitivity factors.²³ Figure 7 shows the V/Zr surface atomic ratio obtained by XPS as a function of the total bulk V/Zr atomic ratio of the catalysts. It can be seen that there is a surface enrichment of V with respect to Zr. The surface V/Zr ratio increases sharply when passing from 0.033 to 0.082. At higher bulk V contents, the surface V/Zr ratio remains

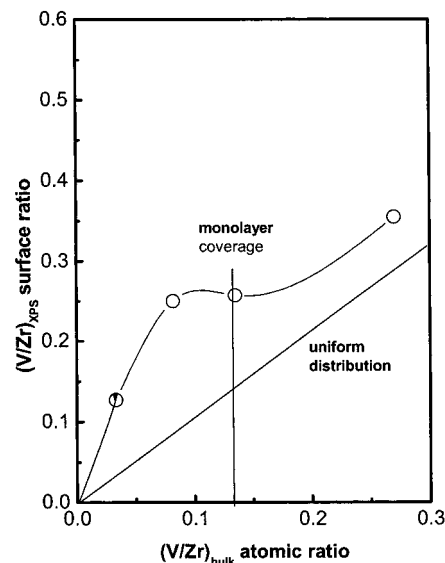


Figure 7. Surface V/Zr atomic ratio obtained by XPS as a function of bulk V/Zr.

Table 3. Distribution of Reaction Products in the *o*-Xylene Oxidation Reaction

	% selectivity ^a at various temperatures (°C) and conversions (%)					
	ZrO ₂		ZrV ₂ O ₇		V/Zr: 0.270	
	350 °C 16.5%	400 °C 25.7%	380 °C 16.9%	440 °C 60.3%	380 °C 63.2%	400 °C 95.5%
phthalic anhydride	5.1	4.4	8.9	22.7	35.6	41.0
CO ₂	18.8	69.9	25.9	28.8	32.0	40.9
CO	0.0	0.0	0.0	9.5	7.4	14.2
maleic anhydride	1.6	1.7	3.2	2.0	2.4	1.7
<i>o</i> -toluic acid	0.0	0.0	4.2	1.1	0.9	0.1
<i>o</i> -tolualdehyde	8.6	12.7	18.8	27.3	13.8	1.4
phthalide	8.4	5.0	6.3	6.6	7.3	0.7
others	57.5	6.3	32.7	2.0	0.6	0.0

^a Selectivity: moles of product / \sum moles of products.

practically constant or increases very little. This indicates that at V/Zr = 0.135 there is an aggregation of vanadium oxide species, mainly as ZrV₂O₇ (XRD and Raman data).

A preliminary screening of the reaction conditions was carried out in order to find the optimum ones. The temperature was varied, and a value was sought that would give a conversion near 100% and good selectivity to phthalic anhydride. It is well-known that at low conversion values selectivity is poor because too many intermediate products are found among the reaction products. By contrast, total conversion conditions must be carefully tuned because they may lead to the deep oxidation of the hydrocarbons to CO and CO₂. This usually happens if the temperature is too high. Some of the results of the screening are reported in Table 3. Some heavy oxidized products such as *o*- and *p*-methyl-diphenyl methanone and *diphenyl* methanone as well as other heavier products with high boiling points have been detected although their proportion is only significant at low *o*-xylene conversion (ZrO₂ at 350 °C and ZrV₂O₇ at 380 °C). This products are indicated as "others" in Table 3. It can be seen that in the case of the catalysts with high V contents there is an increase in conversion and selectivity to phthalic anhydride (selectivity is defined as moles of product / \sum moles of products). This is due to a decrease in the amount of intermediate reaction products, mainly *o*-tolualdehyde. For the V-free support, the increase in temperature produces a small increase in activity although

(40) *Practical Surface Analysis. Auger and X-ray Photoelectron Spectroscopy*; Briggs, D., Seah, M. P., Eds.; John Wiley and Sons: Chichester, 1990.

(41) Nag, N. K.; Chary, K. V. R.; Rao, B. R.; Subrahmanyam, V. S. *Appl. Catal.* **1987**, *31*, 73–85.

(42) Faraldos, M.; Bañares, M. A.; Anderson, J. A.; Hu, H.; Wachs, I. E.; Fierro, J. L. G. *J. Catal.* **1996**, *160*, 214–221.

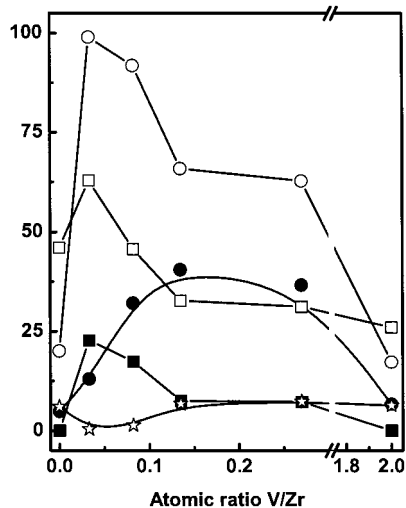


Figure 8. Catalytic activity data for the reaction of *o*-xylene oxidation as a function of the V/Zr bulk atomic ratio: (○) conversion; (●) selectivity to phthalic anhydride; (□) selectivity to CO_2 ; (■) selectivity to CO; (☆) selectivity to phthalide. Reaction temperature was 380 °C.

selectivity to phthalic anhydride decreases due to the formation of CO_2 .

In the case of ZrV_2O_7 , the increase in temperature induces an increase in conversion and also in selectivity to phthalic anhydride, but the catalyst is less active than the catalyst with V/Zr = 0.270 and too many intermediate products are formed. In sum, both the unpromoted support and bulk ZrV_2O_7 have lower conversions and selectivities to phthalic anhydride than the supported V catalyst with V/Zr = 0.270.

Figure 8 shows the results of VO_x/ZrO_2 system for *o*-xylene oxidation to phthalic anhydride at 380 °C. The ZrO_2 support has very low activity. At low vanadium oxide coverage on the ZrO_2 substrate, the system is very active. The conversion of *o*-xylene decreases with VO_x loading. However, selectivity to phthalic anhydride passes through a maximum with VO_x loading. As VO_x loading on ZrO_2 approaches the monolayer, the production of CO and CO_2 decreases continuously and the production of phthalic anhydride increases concomitantly. It appears that the coverage of ZrO_2 support sites by VO_x species prevents nonselective oxidation of the reaction intermediates. The VO_x/TiO_2 system shows the same effect. Thus, the VO_x/TiO_2 catalysts are most efficient at monolayer coverage of VO_x on TiO_2 , since exposed TiO_2 sites lead to CO_x .¹³ The V/Zr = 0.135 and 0.270 catalysts show similar activity and selectivity values: phthalic anhydride is the main reaction product.

Figure 9 plots the conversion and selectivity values versus the acidity of the catalysts, measured as NH_3/m^2 (Table 1). The highest conversion values are afforded by intermediate acidity values, but maximum selectivity values are reached by the samples with the highest and lowest acidity values. Thus, it appears that acidity is not a critical parameter for *o*-xylene oxidation to phthalic anhydride on VO_x/ZrO_2 catalysts.

The poor selectivity to phthalic anhydride of the V_2O_5/ZrO_2 system as compared to the V_2O_5/TiO_2 system is difficult to explain. The properties of ZrO_2 and TiO_2 , and the V species formed, are quite similar. Wachs et al.⁴³ have proposed that in the case of V_2O_5/TiO_2 (anatase) catalysts the dramatic promotional effect of the support is due to the highly active site formed by the bridging

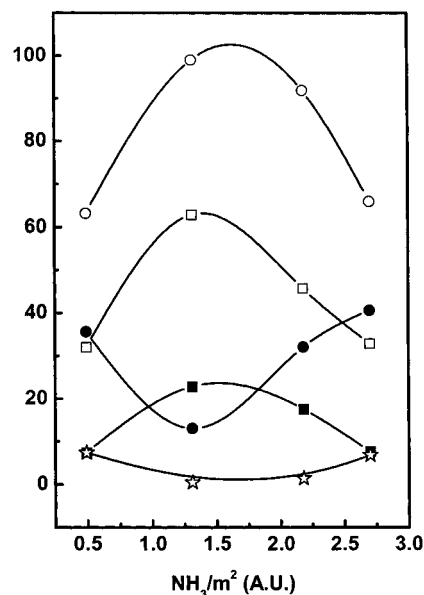


Figure 9. Catalytic activity data for the reaction of *o*-xylene oxidation as a function of acidity (as measured by NH_3/m^2 desorption). Symbols are same as those in Figure 8. Reaction temperature was 380 °C.

oxygen that anchors the surface vanadium oxide species to the titania surface. Furthermore, TiO_2 (anatase) must be covered by a complete monolayer of the surface vanadia species in order to be active and selective for oxidation of *o*-xylene to phthalic anhydride. Exposed titania sites may lead to complete oxidation of C_8 -oxygenates.¹³ On the other hand, catalysts with a high V_2O_5 content show a poorer catalytic performance attributed to the intrinsically lower activity and selectivity of V_2O_5 crystallites formed on the surface, as compared to the activity and selectivity of the vanadium oxide dispersed in monolayer.^{13,14} The oxidation state of vanadium in V_2O_5/TiO_2 catalyst is still a matter of controversy. Some authors consider that vanadium is present only in the form of V^V .¹³ It has also been reported⁴⁴ that fresh V_2O_5/TiO_2 (EUROCAT oxide) has traces of V^{IV} and that the vanadia phase can be partly reduced to V^{IV} .^{14,45} The formation of V^{IV} has been reported to be important when the catalyst is calcined at high temperatures. Vanadium atoms would diffuse into the TiO_2 crystal, which, in turn, would be transformed to the rutile phase.¹⁴

The lower V^{IV}/V_{total} ratio of supported vanadium oxide does induce a change in the redox properties of both systems. Centi et al.^{45,46} have shown that V^V is more selective than V^{IV} . They reported that the presence of V^{IV} on the surface alters the reactivity, leading to a loss of selectivity in active catalysts,⁴⁶ while V^V sites could be involved in oxygen insertion in the activated hydrocarbon and V^{IV} sites would be important for the activation of *o*-xylene. Therefore, the enhanced selectivity in V_2O_5/TiO_2 catalysts can be attributed to a reduction in the amount of V^{IV} species present.² In our case, the decrease in the V^{IV}/V_{total} ratio from catalyst V/Zr = 0.033 to catalyst V/Zr = 0.135 was accompanied by a continuous increase in selectivity to phthalic anhydride. Another factor that can modify the selectivity is the easier reducibility of the TiO_2 -supported V species as compared to the ZrO_2 -supported ones.⁴⁵ On the basis of a reaction taking place through a

(44) Aboukais, A. *Catal. Today* **1994**, *20*, 87–96.

(45) Centi, G.; Giamello, E.; Pinelli, D.; Trifirò, F. *J. Catal.* **1991**, *130*, 220–237.

(46) Centi, G.; Pinelli, D.; Trifirò, F.; Ghosouss, D.; Guelton, M.; Gengembre, L. *J. Catal.* **1991**, *130*, 238–256.

(43) Wachs, I. E. *Chem. Eng. Sci.* **1990**, *45*, 2561–2565.

Mars–van Krevelen mechanism involving a reduction–oxidation cycle of the active species, the V/TiO₂ catalyst should be more active than the V/ZrO₂ system.

Conclusions

It can be concluded that the structure of the V₂O₅/ZrO₂ catalysts studied in this work depends strongly on the V loading. At low V loadings, it mainly disperses as surface vanadium oxide species and the support is transformed from the tetragonal to the monoclinic crystal phase. At monolayer coverage, a ZrV₂O₇ phase is formed through a solid-state reaction between dispersed V₂O₅ and the ZrO₂ substrate upon calcination. Activity tests revealed that V₂O₅/ZrO₂ systems with dominant surface vanadium oxide species are more active for the oxidation of *o*-xylene but

that they have low selectivity to phthalic anhydride, probably due to the contribution of the support. By contrast, samples in which vanadium is almost completely present as ZrV₂O₇, for which XPS revealed some surface V enrichment and lower V^{IV}/V_{total} ratios, display higher selectivity toward phthalic anhydride.

Acknowledgment. C.L.P. thanks the Spanish Ministry of Education for a grant to fund his stay in Spain. This research was partly funded by the EU under Project BE-1169. CICYT Grant IN96-0053 funded the acquisition of the Raman spectrometer. Thanks are due to Dr. M. A. Vicente for XRD experiments.

LA0114631